

SPIN ICE IN A FIELD: QUASI-PHASES AND PSEUDO-TRANSITIONS

*P. N. Timonin**

*Southern Federal University
344090, Rostov-on-Don, Russia*

Received January 14, 2011

Thermodynamics of a short-range model of spin ice magnets in a field is considered in the Bethe–Peierls approximation. The results obtained for [111], [100], and [011] fields agree reasonably well with the existing Monte Carlo simulations and some experiments. In this approximation, all extremely sharp field-induced anomalies are described by analytic functions of temperature and the applied field. In spite of the absence of true phase transitions, the analysis of the entropy and specific heat reliefs over the H – T plane allows discerning “pseudo-phases” with a specific character of spin fluctuations and defining the lines of relatively sharp “pseudo-transitions” between them.

The discovery of spin ice compounds [1, 2] has opened wide perspectives in the studies of real geometrically frustrated magnets, with their reach physics stemming from the macroscopically degenerate ground states. An additional remarkable feature is that these compounds can be described by the relatively simple Ising model with the nearest-neighbor exchange on the pyrochlore lattice. This is due to the lucky chance that strong dipole interactions in these compounds have a negligible effect on the low-energy excitations of the Ising moments directed along the lines connecting the centers of corner-sharing tetrahedra [3]. The low-temperature physics of spin ices can therefore be adequately captured by the short-range Ising model except for the ultra-low temperatures where the equilibrium properties may be unobservable [4].

Such a model predicts the absence of phase transitions in zero field, which agrees with experiments in spin ice compounds [1, 2]. Meanwhile, a wealth of relatively sharp anomalies in the applied magnetic fields H of different directions is observed in their thermodynamic parameters [5–14]. Some of these anomalies are interpreted as field-induced transitions, while others are thought to indicate the crossover between the regions with different types of collective spin fluctuations. The notion of such regions originates from Villain’s idea of low-temperature “spin-liquid” state in frustrated magnets [15], where spin fluctuations are strongly cor-

related, being mostly confined to the ground-state subspace. By contrast, the high-temperature region features uncorrelated spin fluctuations and hence represents a genuine paramagnet. Although there is no true phase transition between paramagnet and spin-liquid state, the temperature dividing these “quasi-phases” can nevertheless be identified, as the temperature T_m of a maximum of specific heat maximum in its temperature dependence $C(T)$ [4]. Indeed, this maximum indicates a relatively sharp decrease in entropy due to the confinement of spin fluctuations at low T . It may be hoped that this definition of T_m can justify the notion of “pseudo-transition” between the “quasi-phases” with different types of spin fluctuations and, in the framework of rigorous theory, may help quantify the regions where various spin-liquid states exist.

Implicitly, the notions of “quasi-phases” and “pseudo-transition” are widely used to heuristically interpret the observed field-induced anomalies of $C(T)$ in spin ices and to identify the regions belonging to different spin-liquid states on the H – T planes [9–13]. Yet it is important to discriminate between the “pseudo-transitions” and the ordinary ones because the microscopic models describing the former would not have any singular point but only the crossover regions. In addition, these crossovers can become progressively sharper at low T and in the vicinity of critical fields, such that the “pseudo-transitions” may look like true transitions in experiments and simulations. The observed sharpening of “pseudo-transitions” gives rise to the

*E-mail: pntim@live.ru

idea that in [111] (Refs. [9–11]), [110] (Refs. [12, 13]), and [100] (Ref. [16]) fields at low temperatures spin ice compounds experience first-order transitions of the “gas–liquid” type, ending up at the critical point at some maximal T . Also from the same sharpening, the notion of the specific “Kasteleyn transition” in the short-range spin ice model in [100] field [17] originated.

Here, we show that most probably, there are no true phase transitions in the short-range spin ice model in [111], [100], and [110] fields and all the observed thermodynamic anomalies can be described by perfectly smooth functions of T and H . Actually, this conclusion can be made on the basis of the existing theoretical results. Indeed, the papers presenting Monte Carlo simulations in the regions of “gas–liquid” [16, 18] and “Kasteleyn” transitions [17] also present the results obtained in the Bethe–Peierls (BP) approximation “corroborating” the numerical results. Both these data show a remarkable agreement with experiments [6, 9–11], but BP results describe extremely sharp anomalies with perfectly smooth functions. Taking this fact seriously may tell us that we are actually dealing with the “pseudo-transitions” and their sharpening at low T .

We show explicitly how the BP approximation in the short-range spin ice model can describe very sharp field-induced anomalies with analytic functions of T and H . In the BP approach, the sharp anomalies at low T are only the reflections of true first-order transitions that occur at $T = 0$ and some critical fields. In view of the high precision with which the BP approximation can reproduce the nominally exact results [16–18] as well as experimental data [6–13] and quite clear physics underlying the origin of the anomalies, we can suppose that BP’s “pseudo-transitions” are not artefacts of the approximation but the intrinsic feature of the model.

1. SPIN ICE IN THE BETHE–PEIERLS APPROXIMATION

Magnetic ions in spin ice are placed on the pyrochlore lattice consisting of corner-sharing tetrahedra; a fragment of the lattice is shown in Fig. 1. Strong anisotropy allows only two directions of magnetic moments along the local easy axis connecting the site with the centers of tetrahedra. Therefore, the magnetic state is defined by Ising spins σ_α on the sites. Considering four sites belonging to the central tetrahedron in Fig. 1, we define their easy axes by the unit vectors shown in this figure:

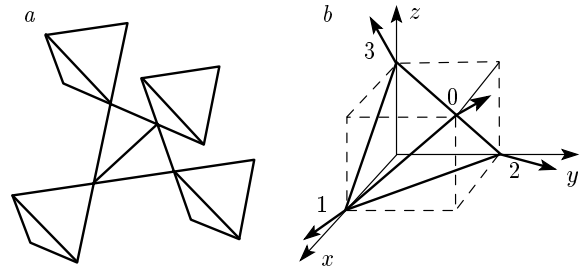


Fig. 1. Fragment of a pyrochlore lattice (a) and the vectors defining the directions of the easy axes on their sites (b)

$$\begin{aligned} \mathbf{e}_0 &= (\hat{x} + \hat{y} + \hat{z}) / \sqrt{3}, & \mathbf{e}_1 &= (\hat{x} - \hat{y} - \hat{z}) / \sqrt{3}, \\ \mathbf{e}_2 &= (-\hat{x} + \hat{y} - \hat{z}) / \sqrt{3}, & \mathbf{e}_3 &= (-\hat{x} - \hat{y} + \hat{z}) / \sqrt{3}. \end{aligned} \quad (1)$$

Here, \hat{x} , \hat{y} , and \hat{z} are the unit vectors along the coordinate axes. Then the magnetic moments of the sites are

$$\mathbf{m}_\alpha = \mathbf{e}_\alpha \sigma_\alpha \quad (2)$$

and the effective Hamiltonian for the tetrahedron in an external field \mathbf{H} is [14]

$$\mathcal{H}(\sigma) = \frac{J}{2} \left(\sum_{\alpha=0}^3 \sigma_\alpha \right)^2 - \sum_{\alpha=0}^3 \sigma_\alpha H_\alpha, \quad H_\alpha \equiv \mathbf{H} \cdot \mathbf{e}_\alpha. \quad (3)$$

With definition (1), the identities

$$\sum_{\alpha=0}^3 \mathbf{e}_\alpha = 0, \quad \mathbf{e}_\alpha \cdot \mathbf{e}_\beta = -\frac{1}{3}, \quad \alpha \neq \beta, \quad (4)$$

hold, and $\sigma_\alpha = 1$ corresponds to the “out” moment.

The BP approximation for the pyrochlore lattice [17] assumes that the effective fields acting on the sites of a given tetrahedron (say, the central one in Fig. 1a) from all other sites are the same as those acting on its nearest neighbours (outer sites in Fig. 1a) from all other sites except those of the given tetrahedron. This field equivalence does not actually hold on the pyrochlore lattice due to the correlations arising from the closed loops of tetrahedra. But it becomes exact on the variant of the hierarchical Bethe lattice built from the corner-sharing tetrahedra [17]. We can obtain it from the cluster in Fig. 1a attaching a tetrahedron to each outer site and then endowing each of the new outer sites with a new tetrahedron, and so on. The process is illustrated by the planar graph in Fig. 2a, where tetrahedra are projected to the squares with the numbers on their sites indicating the orientations of easy axes.

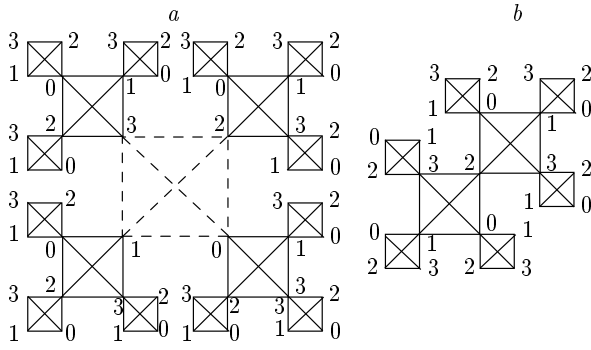


Fig. 2. *a)* Fragment of a Bethe lattice built hierarchically via addition of new tetrahedra to the outer sites. The lattice can be viewed as consisting of four trees connected by the bonds of the central tetrahedron (dashed line). The numbers indicate the directions of easy axes of the sites, *b)* the same lattice can be obtained from two trees via merging their root sites

As Fig. 2*a* shows, we can consider such a Bethe lattice as consisting of four α -trees with $\alpha = 0, 1, 2, 3$ denoting their root sites, which are connected by the bonds of the central tetrahedra. Alternatively, we can obtain the lattice from two α -trees merging their root sites (cf. Fig. 2*b*). Hence, there are two ways to construct the free energy of the Bethe lattice with the partial partition functions $Z_\alpha(\sigma_\alpha, N)$ for the N -site α -trees summed over all spins except the root one. Using the first representation of the Bethe lattice, we have the free energy

$$\Phi_4 = -T \ln \text{Tr}_\alpha e^{-\beta \mathcal{H}(\sigma)} \prod_{\alpha=0}^3 Z_\alpha(\sigma_\alpha, N), \quad (5)$$

where $\beta = T^{-1}$, $\mathcal{H}(\sigma)$ is defined in Eq. (3), and Tr_σ denotes the summation over σ_α , $\alpha = 0, 1, 2, 3$. In the other representation, we obtain the free energies

$$\Phi_{2\alpha} = -T \ln \text{Tr}_{\sigma_\alpha} e^{h_\alpha \sigma_\alpha} Z_\alpha^2(\sigma_\alpha, N), \quad h_\alpha \equiv \beta H_\alpha. \quad (6)$$

Assuming the finite correlation range in our system we have in the thermodynamic limit, $N \rightarrow \infty$,

$$\Phi_4 \rightarrow 4NF + 4SG, \quad \Phi_{2\alpha} \rightarrow (2N - 1)F + 2SG,$$

where F is the (internal) free energy per site in this limit, S is the number of surface sites in a tree and G is the density of the surface contribution to the full potential. $2N - 1$ in the second relation appears because we have merged two root sites into one.

The peculiarity of Bethe lattices having formally the infinite spatial dimension consists in the finite ratio S/N at $N \rightarrow \infty$. In our lattice $S/N \rightarrow 2/3$ and

we cannot neglect the surface contribution to the full potential. Yet this circumstance does not prevent the determination of the free energy per site F from Φ_4 and $\Phi_{2\alpha}$ as we can choose their linear combination where the surface terms conceal each other. Thus we have

$$F = \frac{1}{4} \lim_{N \rightarrow \infty} \left(2\Phi_4 - \sum_{\alpha=0}^3 \Phi_{2\alpha} \right). \quad (7)$$

We can also represent $Z_\alpha(\sigma_\alpha, N)$ in Eqs. (5) and (6) as

$$Z_\alpha(\sigma_\alpha, N) = A_\alpha(N) e^{x_\alpha \sigma_\alpha},$$

where $x_\alpha T$ has the meaning of the effective magnetic fields exerted on the sites of the central tetrahedron by the other spins in the lattice. From (3) and (5)–(7), introducing the new variables $f_\alpha = x_\alpha + h_\alpha$ instead of x_α , we then obtain

$$F = \frac{T}{4} \sum_{\alpha=0}^3 \ln [2 \text{ch}(2f_\alpha - h_\alpha)] - \frac{T}{2} \ln 2Z(\mathbf{f}), \quad (8)$$

$$Z(\mathbf{f}) \equiv \frac{1}{2} \text{Tr}_\sigma w(\sigma, \mathbf{f}),$$

$$w(\sigma, \mathbf{f}) = \exp \left[-\frac{K}{2} \left(\sum_{\alpha=0}^3 \sigma_\alpha \right)^2 + \sum_{\alpha=0}^3 f_\alpha \sigma_\alpha \right], \quad (9)$$

$$K \equiv \beta J.$$

Owing to the form of Eq. (7), the resulting expression for F depends only on the parameters f_α . The equations for f_α can be obtained from the condition that they provide a minimum of F ,

$$\frac{\partial F}{\partial f_\alpha} = 0, \quad \sum_{\alpha, \beta} c_\alpha c_\beta \frac{\partial^2 F}{\partial f_\alpha \partial f_\beta} > 0 \quad \text{for all } \mathbf{c}, \quad (10)$$

or

$$\text{th}(2f_\alpha - h_\alpha) = \langle \sigma_\alpha \rangle_w, \quad (11)$$

where the angular brackets with the “w” subscript denote the average with the distribution function $w(\sigma, \mathbf{f})$ from Eq. (9). Alternatively, we can obtain the same equations (11) from recursion relations for $Z_\alpha(\sigma, N)$. For the Hessian in Eq. (10), we obtain

$$\frac{\partial^2 F}{\partial f_\alpha \partial f_\beta} = \delta_{\alpha\beta} [1 - \langle \sigma_\alpha \rangle_w^2] - \frac{1}{2} \langle \sigma_\alpha \sigma_\beta \rangle_w + \frac{1}{2} \langle \sigma_\alpha \rangle_w \langle \sigma_\beta \rangle_w. \quad (12)$$

The standard derivation of Eqs. (11) does not yield a positive definiteness of the Hessian which causes no

problems when these equations have a unique solution. Otherwise, we would have to choose among the solutions, the natural choice being the one that provides the global free energy minimum.

With f_α obtained from Eqs. (11), we can fully describe the spin ice thermodynamics in the BP approximation. For the equilibrium values of spins, $\langle\sigma_\alpha\rangle$, we use the lattice representation in Fig. 2b to obtain

$$\langle\sigma_\alpha\rangle = \frac{\text{Tr}_{\sigma_\alpha} \sigma_\alpha Z_\alpha^2(\sigma_\alpha) e^{h_\alpha \sigma_\alpha}}{\text{Tr}_{\sigma_\alpha} Z_\alpha^2(\sigma_\alpha) e^{h_\alpha \sigma_\alpha}} = \text{th}(2f_\alpha - h_\alpha). \quad (13)$$

According to Eq. (2), the equilibrium magnetization per spin is then given by

$$\langle\mathbf{m}\rangle = \frac{1}{4} \sum_{\alpha=0}^3 \mathbf{e}_\alpha \langle\sigma_\alpha\rangle = \frac{1}{4} \sum_{\alpha=0}^3 \mathbf{e}_\alpha \text{th}(2f_\alpha - h_\alpha). \quad (14)$$

Also from (8)–(11), we obtain the equilibrium entropy

$$S = -\frac{\partial F}{\partial T} = -\beta F - \frac{1}{4} \sum_{\alpha=0}^3 h_\alpha \langle\sigma_\alpha\rangle + \frac{K}{Z(\mathbf{f})} (Z_1(\mathbf{f})e^{-2K} + 4Z_2(\mathbf{f})e^{-8K}). \quad (15)$$

Here, we introduce the quantities

$$Z_n(\mathbf{f}) = \frac{1}{2} \text{Tr}_\sigma \left\{ e^{\sum_{\alpha=0}^3 \sigma_\alpha f_\alpha} \times \delta \left[\left(\sum_{\alpha=0}^3 \sigma_\alpha \right)^2, 4n^2 \right] \right\}, \quad n = 0, 1, 2, \quad (16)$$

which define the contributions to $Z(\mathbf{f})$ in (8) from the groups of states with equal exchange energies:

$$Z(\mathbf{f}) = \sum_{n=0}^2 Z_n(\mathbf{f}) e^{-2n^2 K}. \quad (17)$$

Hence, $Z_0(\mathbf{f})$ corresponds to the contributions of spin ice states (two in, two out), $Z_1(\mathbf{f})e^{-2K}$ describes the contributions of (three in, one out) and (three out, one in) states, and $Z_2(\mathbf{f})e^{-8K}$ results from all in and all out states. Explicit expressions for $Z_n(\mathbf{f})$ are

$$\begin{aligned} Z_0(\mathbf{f}) &= \text{ch}(f_0 + f_1 - f_2 - f_3) + 2 \text{ch}(f_0 - f_1) \text{ch}(f_2 - f_3), \\ Z_1(\mathbf{f}) &= \sum_{\alpha=0}^3 \text{ch} \left(\sum_{\beta=0}^3 f_\beta - 2f_\alpha \right), \\ Z_2(\mathbf{f}) &= \text{ch} \left(\sum_{\alpha=0}^3 f_\alpha \right). \end{aligned} \quad (18)$$

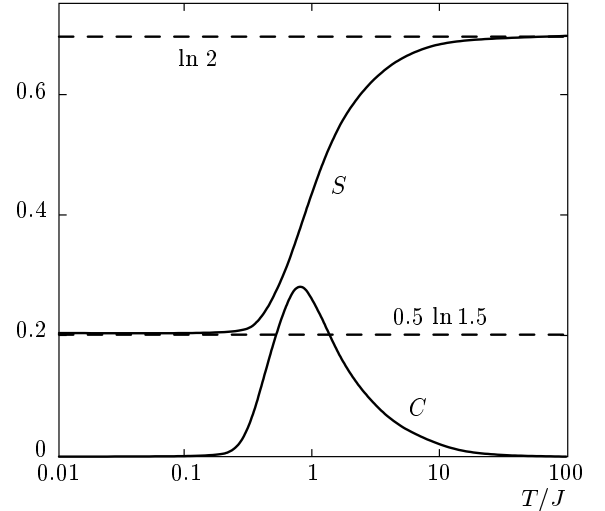


Fig. 3. Temperature dependence of S and C in zero field. A logarithmic scale is chosen on the T axis

From (17) and (18), we can also obtain the explicit form of equations of state (11) as

$$\text{th}(2f_\alpha - h_\alpha) = \frac{\partial \ln Z(\mathbf{f})}{\partial f_\alpha}. \quad (19)$$

Further differentiations of Eqs. (14) and (15) can yield the tensor of magnetic susceptibilities and specific heat.

We have a quite simple theory of spin ice thermodynamics consisting essentially of Eqs. (8) and (9). This theory can describe all intricate features of this strongly frustrated system behavior in various fields, as we show below. To begin, we can easily find that in a zero field, S in Eq. (15) gives the Pauling value of the residual entropy at $T = 0$ [19]:

$$S_P = \frac{1}{2} \ln \frac{3}{2} \approx 0.2.$$

Indeed, at $H = 0$, $f_\alpha = 0$, and $Z_0 = 3$, $Z_1 = 4$, $Z_2 = 1$, and hence

$$S(T) = -\frac{1}{2} \ln 2 + \frac{1}{2} \ln(3 + 4e^{-2K} + e^{-8K}) + 4K \frac{e^{-2K} + e^{-8K}}{3 + 4e^{-2K} + e^{-8K}}.$$

Therefore, $S(0) = S_P$ at $T = 0$ ($K = \infty$), while $S(\infty) = \ln 2$ at $T = \infty$ ($K = 0$). For the specific heat, we obtain

$$C = T \frac{\partial S}{\partial T} = \frac{24K^2 e^{-2K} (1 - 2e^{-2K} + 3e^{-4K})}{(3 + e^{-2K} - e^{-4K} + e^{-6K})^2}.$$

The temperature behavior of S and C is shown in Fig. 3. It illustrates the notions of “quasi-phases” and

“pseudo-transition”. The function S exhibits a broad crossover between Pauling and paramagnetic values, but below $T_m \approx 0.8J$, where C has a maximum, we have a “spin ice liquid”, where the local spin configurations are mainly “two in, two out”, while above T_m , they are almost uncorrelated and we have a “paramagnetic quasi-phase”.

2. SPIN ICE IN THE [111] FIELD

For $\mathbf{H} = H\mathbf{e}_0$, we have

$$h_0 = h, \quad h_1 = h_2 = h_3 = -h/3, \quad h \equiv \beta H$$

and the solution of Eq. (19) has the form

$$f_0 = x, \quad f_1 = f_2 = f_3 = -y.$$

It then follows from (19) that

$$\begin{aligned} \text{th}(2x - h) &= \frac{\partial \ln Z(x, y)}{\partial x}, \\ 3 \text{th}\left(2y - \frac{h}{3}\right) &= -\sum_{i=1}^3 \frac{\partial \ln Z(\mathbf{f})}{\partial f_i} = \frac{\partial \ln Z(x, y)}{\partial y}, \end{aligned} \quad (20)$$

where $Z(x, y)$ is given by Eq. (17) with

$$\begin{aligned} Z_0(x, y) &= 3 \text{ch}(x + y), \\ Z_1(x, y) &= \text{ch}(x + 3y) + 3 \text{ch}(x - y), \\ Z_2(x, y) &= \text{ch}(x - 3y). \end{aligned} \quad (21)$$

Also from (4) and (14), we have

$$\langle \mathbf{m} \rangle = \frac{\mathbf{e}_0}{4} \left[\text{th}(2x - h) + \text{th}\left(2y - \frac{h}{3}\right) \right]. \quad (22)$$

We first consider the case of low temperatures and moderate fields

$$T \ll J, \quad H \leq J.$$

As we show below, we can then drop the contributions to Z that are proportional to Z_1 and Z_2 , and therefore Eqs. (20) become

$$\text{th}(2x - h) = 3 \text{th}\left(2y - \frac{h}{3}\right) = \text{th}(x + y). \quad (23)$$

Hence, we have

$$\begin{aligned} x &= y + h, \\ m = |\langle \mathbf{m} \rangle| &= \text{th}\left(2y - \frac{h}{3}\right) = \frac{1}{\sqrt{1 + 3t^2} + 1}, \\ t &\equiv \text{th}\left(\frac{4}{3}h\right). \end{aligned} \quad (24)$$

Using this m , we can express other thermodynamic quantities as

$$-\beta F = \frac{1}{2} \ln \frac{3}{2} + \frac{1}{8} \ln \frac{(1 - m^2)^3}{1 - 9m^2},$$

$$\begin{aligned} S = -\beta F - hm &= \frac{1}{2} \ln \frac{3}{2} + \\ &+ \frac{3}{8} [(1 - m) \ln(1 - m) + (1 + m) \ln(1 + m)] - \\ &- \frac{1}{8} [(1 + 3m) \ln(1 + 3m) + (1 - 3m) \ln(1 - 3m)], \end{aligned} \quad (25)$$

$$\chi' \equiv T\chi = \frac{\partial m}{\partial h} = \frac{2}{3} \frac{(1 - m^2)(1 - 9m^2)}{1 + 3m^2}, \quad C = h^2 \chi'.$$

The relation for the specific heat C follows from the equation

$$\frac{\partial \beta F}{\partial h} = -m \quad (26)$$

and the scaling form of βF , which depends only on $h = H/T$. Due to this scaling, the above quantities are constant along the lines $H = cT$ and have different limit values at $H = T = 0$ along these lines. In particular, at $H = 0$, we have

$$m = 0, \quad S = S_P, \quad \chi' = \frac{2}{3}, \quad C = 0, \quad (27)$$

while at $T = 0$,

$$m = \frac{1}{3}, \quad S = \frac{1}{4} \ln \frac{4}{3} \approx 0.072, \quad \chi' = C = 0. \quad (28)$$

Here, the entropy value is reduced with respect to S_P because of partial lifting of the ground state degeneracy in the [111] field. This fixes the “out” direction for the 0 spin, while three others can freely choose which one of them is to also point out to obey the ice rule. This phase corresponds to a “kagome ice” state in the original pyrochlore lattice [18].

Following [19], we first consider the spins as belonging to $N/4$ independent tetrahedra. We then have $\Gamma_0 = 3^{N/4}$ states for the spins. Turning to the $N/4$ bond tetrahedra connecting the independent ones, we then see that their free (1, 2, 3) sites have $\sigma = 1$ with the probability $p_+ = 1/3$ and $\sigma = -1$ with the probability $p_- = 2/3$. Therefore, the average number of favorable 3-spin states (two in, one out) per such tetrahedron is $3p_+p_-^2 = 4/9$ and the total number of states $\Gamma = \Gamma_0(4/9)^{N/4} = (4/3)^{N/4}$ gives the value of $S = N^{-1} \ln \Gamma$ in Eq. (28). We thus see that the Pauling–Anderson entropy estimates [19] are exact in the BP approximation.

The behavior of thermodynamic variables near the point $H = T = 0$, given by Eqs. (25), is shown in Fig. 4.

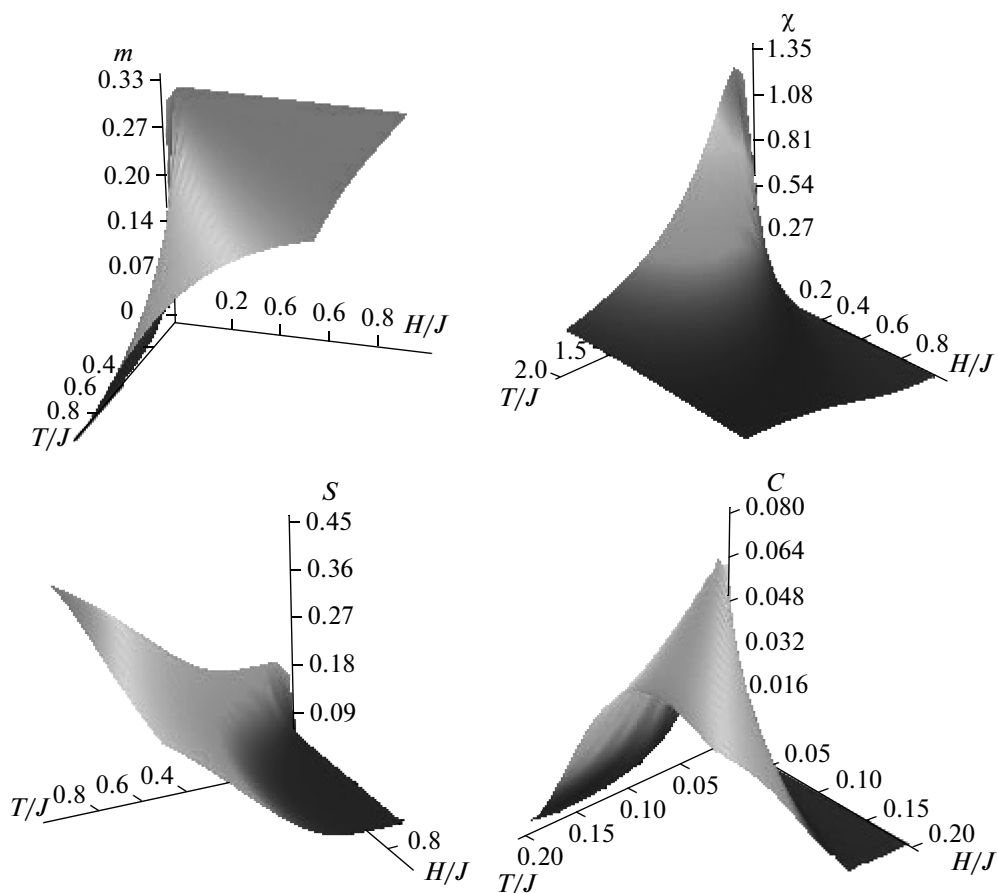


Fig. 4. Field and temperature dependences of thermodynamic variables near $H = T = 0$ in a $[111]$ field

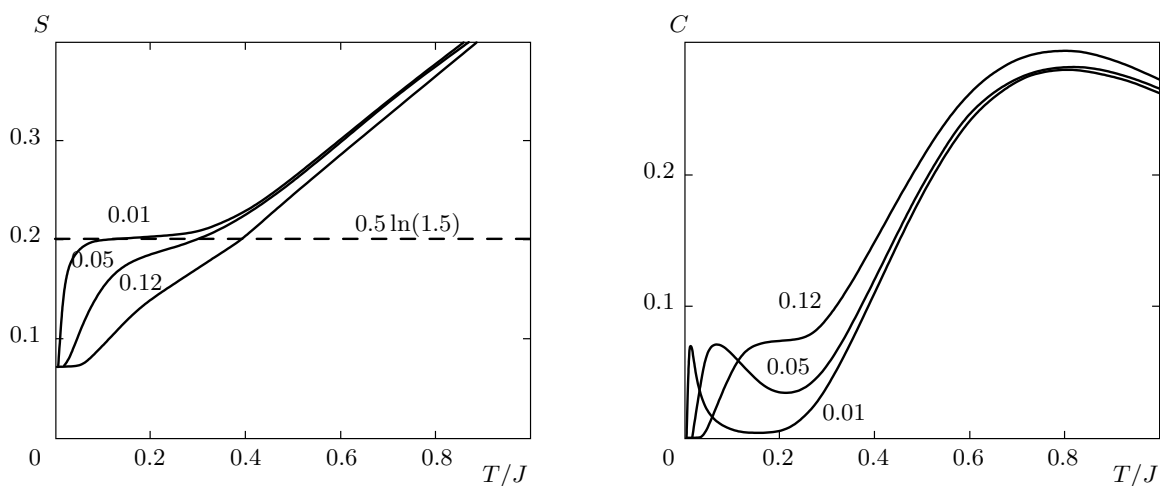


Fig. 5. Temperature dependences of S and C at $T \leq J$ for $H \ll J$, $\mathbf{H} \parallel [111]$. The values of H/J are shown near the curves. The low- T peak of C defines a quasi-transition between the “kagome ice” state with $S \approx 0.072$ to the spin ice state with S close to the Pauling entropy $S_P \approx 0.2$ (dashed line)

The S and C temperature dependences in the broader range $T \leq J$ for $H \ll J$ obtained via numerical solution of the equations of state are presented in Fig. 5. We note the appearance of an additional low- T peak in $C(T)$ at $H \approx 0.7T$ designating a pseudo-transition between the “kagome ice” and ordinary spin ice states.

We can now assess the range of validity of the above analytic results. We have assumed that

$$\varepsilon \equiv \frac{Z_1(x, y)e^{-2K} + Z_2(x, y)e^{-8K}}{Z_0(x, y)} \ll 1.$$

This condition can be violated as $h \rightarrow \infty$ when $x, y \rightarrow \infty$. Indeed, we then have $\varepsilon \sim e^{2(y-K)}$, and therefore the above results hold for $y < K$. From (24), we have $y \approx h/6$ as $h \rightarrow \infty$, and the validity condition for $T \ll J$ is $H < 6J$.

Hence, for $T \ll J$ and $H \geq 6J$, we cannot ignore Z_1 and Z_2 . But analytic results can be also readily obtained in this case. Here, $h \rightarrow \infty$ and we can assume that $x \rightarrow \infty$, and therefore the second equation in (20) becomes

$$\text{th} \left(2y - \frac{h}{3} \right) = \frac{1 + e^{2(y-K)}}{3 + e^{2(y-K)}}.$$

This is actually the quadratic equation

$$u^2 - \lambda u - 2 = 0, \quad u \equiv e^{2y-h/3}, \quad \lambda \equiv e^{h/3-2K}. \quad (29)$$

Therefore,

$$u \equiv e^{2y-h/3} = \frac{1}{2} \left(\lambda + \sqrt{\lambda^2 + 8} \right). \quad (30)$$

From the first equation in (20), we obtain the exact relation

$$e^{2x} = e^{2(y+h)} \frac{\zeta(y, K)}{\zeta(-y, K)}, \quad (31)$$

$$\zeta(y, K) = 3 + e^{2(y-K)} + 3e^{-2(K+y)} + e^{-4(2K+y)}.$$

It follows that always $2x - h \rightarrow \infty$ contrary to $2y - h/3$, and hence, according to (22),

$$m \equiv |\langle \mathbf{m} \rangle| = \frac{1}{4} \left[1 + \text{th} \left(2y - \frac{h}{3} \right) \right] = \frac{\lambda + \sqrt{\lambda^2 + 8}}{\lambda + 3\sqrt{\lambda^2 + 8}}. \quad (32)$$

Again using $2x - h \rightarrow \infty$ and Eqs. (30) and (32), we can express thermodynamic quantities in terms of the magnetization as

$$-\beta F = \frac{1}{2} \ln 2 + \frac{1}{4} \ln \frac{m^2}{1-2m} + \frac{h}{3},$$

$$S = \frac{1}{2}(2-3m) \ln 2 + \frac{3}{2} m \ln m - \frac{3}{4}(1-2m) \ln(1-2m) - (3m-1) \ln(3m-1), \quad (33)$$

$$\chi' = \frac{\partial m}{\partial h} = \frac{2}{3} \frac{(3m-1)(1-2m)}{1-m}, \quad C = (h-6K)^2 \chi'.$$

Hence, at $T \ll J \leq H$, the scaling dependence on the single parameter $(H - H_c)/T$, $H_c \equiv 6J$, also holds. Here, thermodynamic quantities are constant along the straight lines emerging from the point $T = 0$, $H = H_c$. At this point, spin ice undergoes a first-order phase transition from the degenerate “kagome ice” phase to the completely ordered “three in, one out” phase. At $T = 0$, we have

$$\begin{aligned} H < H_c, \quad m &= \frac{1}{3}, \quad S = \frac{1}{4} \ln \frac{4}{3} \approx 0.072, \\ &\quad \chi = C = 0, \\ H = H_c, \quad m &= \frac{2}{5}, \quad S = \frac{1}{4} \ln \frac{16}{5} \approx 0.29, \\ &\quad \chi' = \frac{2}{45}, \quad C = 0, \\ H > H_c, \quad m &= \frac{1}{2}, \quad S = \chi = C = 0. \end{aligned} \quad (34)$$

The large value of S at $H = H_c$ is due to the degeneracy between the configurations of the adjoint phases. We also note that the results for $H < H_c$ coincide with the $T = 0$ results in Eq. (28) valid down to $H = 0$. Hence, at $T = 0$ and $0 < H < H_c$, we have plateaus in field dependences of S and m , which are also seen at low $T < J$ (see Fig. 6). They also have crossing points at $H = H_c$ due to scaling, in agreement with experiments [6, 11] and simulations [18].

Figure 7 shows the behavior of thermodynamic variables at high T and H . The location of specific heat ridges on the H - T plane is summarized in Fig. 8. They are used to define the regions of spin ice, kagome ice, and paramagnetic and completely ordered (“saturated”) quasi-phases. However, the attribution of some definite spin-liquid quasi-phase to the central region in Fig. 8 seems to be less appropriate because it is hard to describe the nature of collective excitations for the whole vast H and T ranges here. The experimental data on C in a [111] field [8–10] show only a vague resemblance to the present results. Accordingly, the phase diagram in Fig. 8 differs essentially from the experimental ones [9, 11].

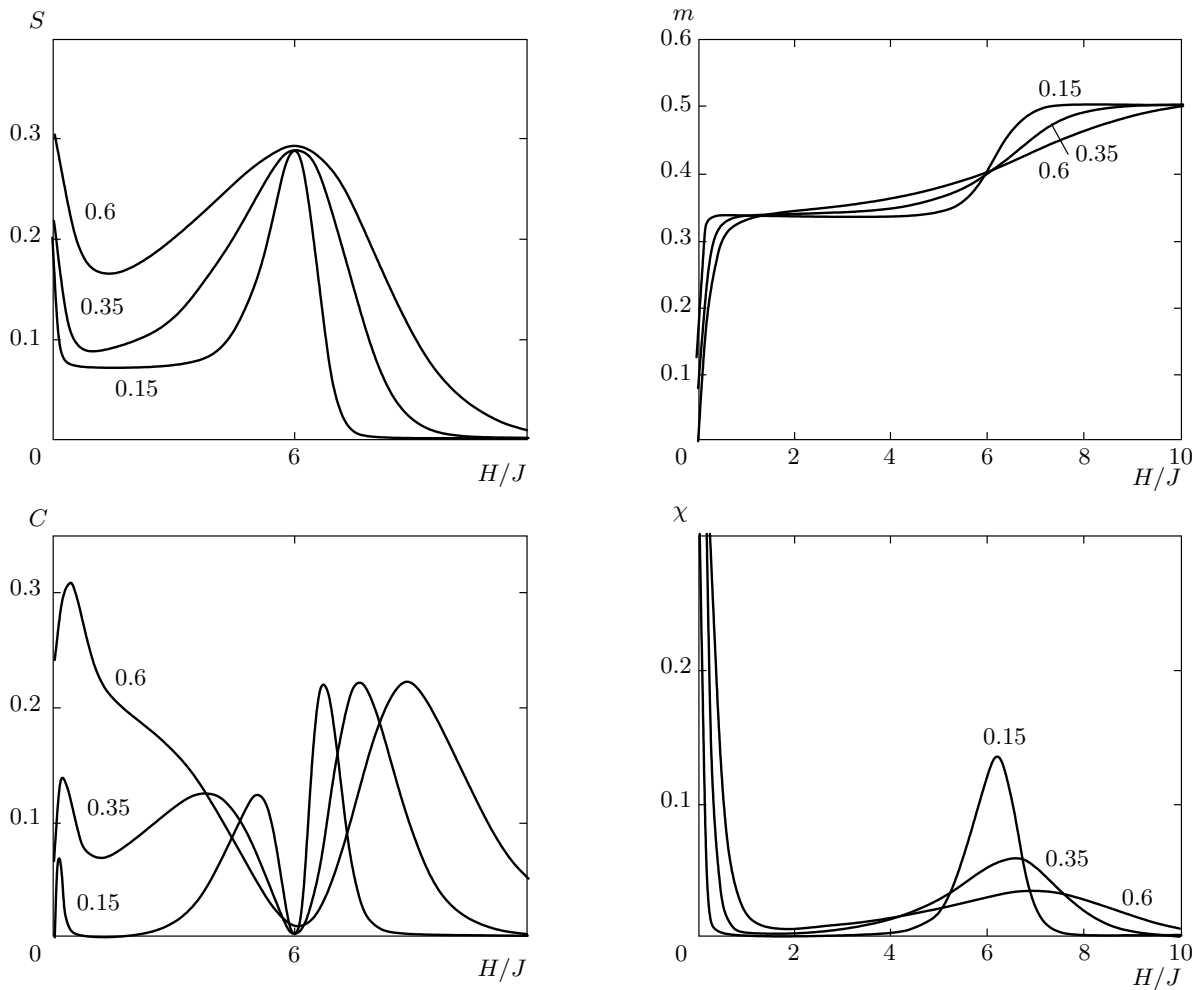


Fig. 6. Field dependences of thermodynamic variables, $T < J$, $\mathbf{H} \parallel [111]$. The values of T/J are shown near the curves

3. SPIN ICE IN THE [100] FIELD

For $\mathbf{H} = H\mathbf{e}_x$, we have

$$h_0 = h_1 = h/\sqrt{3}, \quad h_2 = h_3 = -h/\sqrt{3}, \quad h \equiv \beta H$$

and hence one of the six spin ice configurations (0, 1 spins out, 2, 3 spins in) becomes preferable in this field. The ground state degeneracy is therefore completely lifted and we should have $S = 0$ at $T = 0$. Because $S = S_P$ at $H = 0$ and low T , the increase in the field may result in a “pseudo-transition” from the spin ice to the ordered “saturated” state. Indeed, it shows up in simulations [16, 17] and is extremely sharp at $T \ll J$, which allows defining the transition point as [17]

$$H_c = T \frac{\sqrt{3}}{2} \ln 2 \approx 0.6T. \tag{35}$$

This sharpness results from the existence of specific string excitations with a unique free-energy gap, which

they can overcome at $H < H_c$ [17]. However, we show here that this is only a “pseudo-transition” and its sharp anomalies can be described in the BP approximation with perfectly smooth functions.

The solution of Eq. (19) is given by $f_0 = f_1 = -f_2 = -f_3 = x$, whence

$$\langle \mathbf{m} \rangle = \frac{\mathbf{e}_x}{\sqrt{3}} \operatorname{th} \left(2x - \frac{h}{\sqrt{3}} \right). \tag{36}$$

It follows from (17)–(19) that

$$\begin{aligned} Z(x) &= 2 + \operatorname{ch} 4x + 4e^{-2K} \operatorname{ch} 2x + e^{-8K}, \\ Z(x) \operatorname{th} \left(2x - \frac{h}{\sqrt{3}} \right) &= \operatorname{sh} 4x + 2e^{-2K} \operatorname{sh} 2x. \end{aligned} \tag{37}$$

The last equation is actually an algebraic fourth-order equation for $\nu = \exp(-2x)$,

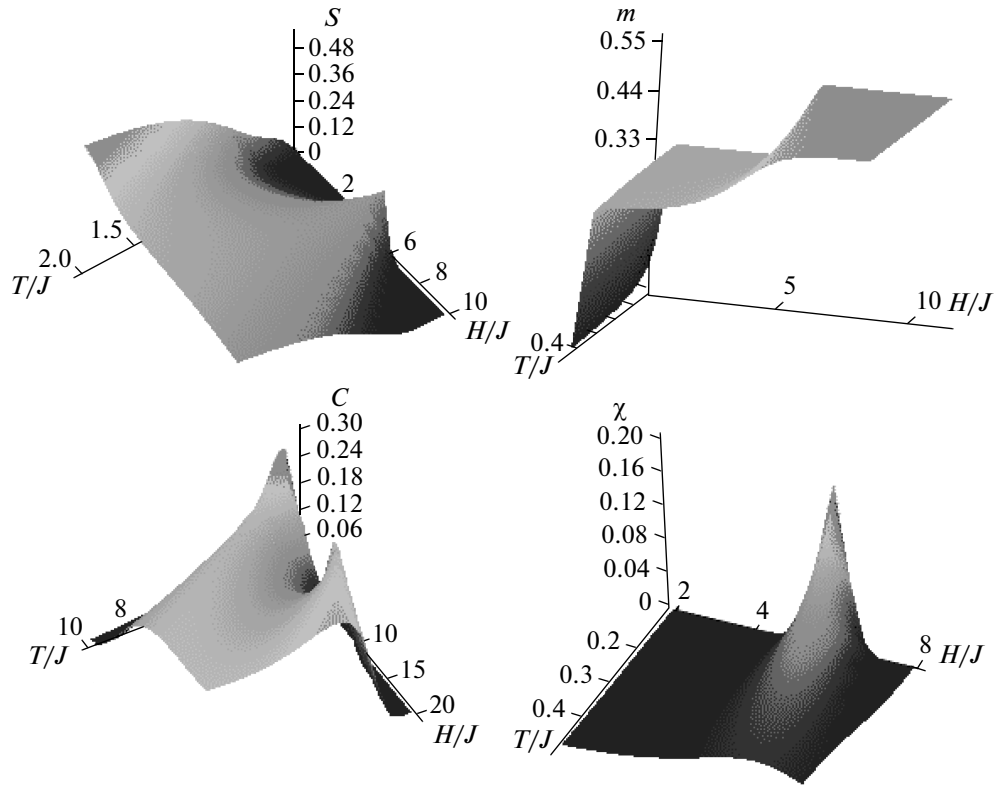


Fig. 7. Thermodynamic variables at high T and H , $\mathbf{H} \parallel [111]$

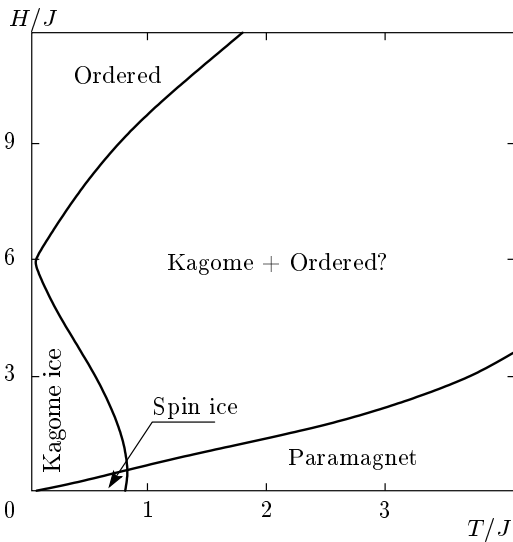


Fig. 8. Quasi-phases and the lines of pseudo-transitions between them for a $[111]$ field

$$av^4 + (2 + a^4 - b)v^3 + 3a(1 - b)v^2 + (1 - 2b - a^4b)v = ab, \quad (38)$$

$$a \equiv \exp(-2K), \quad b \equiv \exp\left(-\frac{2}{\sqrt{3}}h\right).$$

In the interval $0 < \nu < 1$, it has a unique solution that depends analytically on H and T at $T > 0$. Finding the solution numerically, we obtain the thermodynamic quantities as functions of H and T . The results are shown in Figs. 9 and 10. Quite remarkably, at $T \ll J$, we see absolutely sharp anomalies that can be easily mixed up with the genuine phase transitions. But in the present theory, they are only sharp crossovers; the genuine first-order transition takes place only at $T = H = 0$.

To show this, we assume that $T \ll J$ and determine the behavior of ν as $a \rightarrow 0$. We can simplify Eq. (38) to

$$(2 - b)\nu^3 + (1 - 2b)\nu = ab. \quad (39)$$

As $a \rightarrow 0$, we have

$$b < \frac{1}{2}, \quad \nu \rightarrow 0; \quad b = \frac{1}{2}, \quad \nu = \left(\frac{a}{3}\right)^{1/3};$$

$$b > \frac{1}{2}, \quad \nu \rightarrow \sqrt{\frac{2b-1}{2-b}}.$$

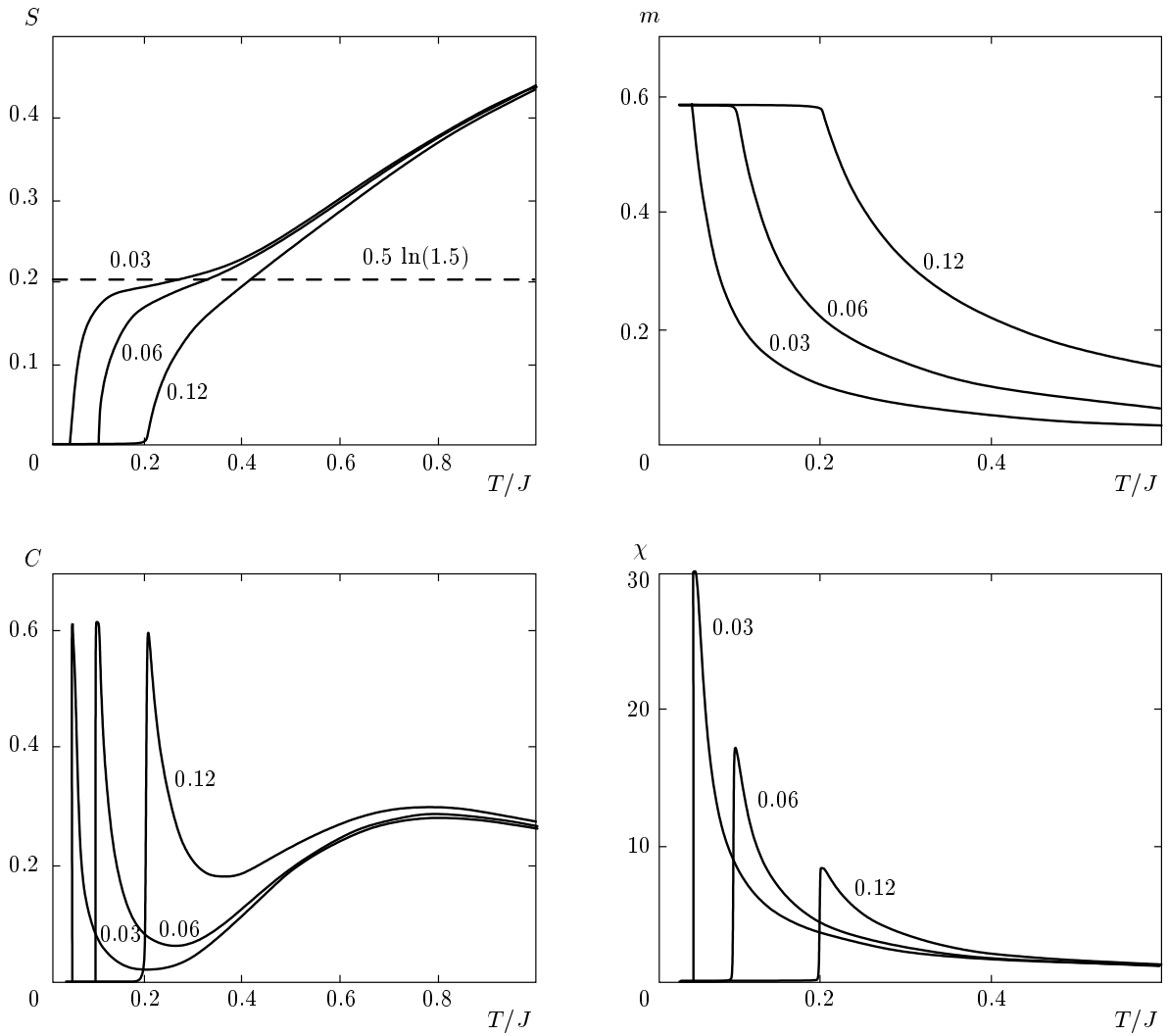


Fig. 9. Temperature dependences of thermodynamic variables in a low [100] field. The values of H/J are shown near the curves. The peaks of C and χ define the Kasteleyn pseudo-transition from the ordered quasi-phase to the spin ice phase with S close to $S_P = 0.5 \ln(1.5)$ (dashed line)

Hence, as $a \rightarrow 0$, $\nu = \nu(b)$ is very close to its limit function

$$\nu = \sqrt{\frac{2b-1}{2-b}} \vartheta(2b-1), \quad (40)$$

differing from it by a small amount of the order of $a^{1/3} = e^{-2K/3}$. We can therefore describe the low-temperature thermodynamics very precisely with the singular $\nu = \nu(b)$ from Eq. (40). Its singular point

$$b \equiv e^{-2H/\sqrt{3}T} = \frac{1}{2}$$

coincides with the critical field H_c in (35), below which the string fluctuations develop in the original pyrochlore structure [17].

At $H > H_c$ ($b < 1/2$), we thus have

$$x = \infty, \quad m = \frac{1}{\sqrt{3}} \approx 0.58, \quad S = C = \chi = 0,$$

and at $H < H_c$ ($b > 1/2$), we obtain

$$\begin{aligned} -\beta F &= \frac{1}{2} \ln \frac{3b}{4b-b^2-1}, \\ S = -\beta F - hm &= \frac{1}{2} \ln \frac{3}{4b-b^2-1} - \frac{2h}{\sqrt{3}} \frac{b(2-b)}{4b-b^2-1}, \\ m &= \frac{1}{\sqrt{3}} \frac{1-b^2}{4b-b^2-1}, \\ \chi' \equiv T\chi &= \frac{8}{3} b \frac{1-b+b^2}{(4b-b^2-1)^2}, \quad C = h^2 \chi'. \end{aligned}$$

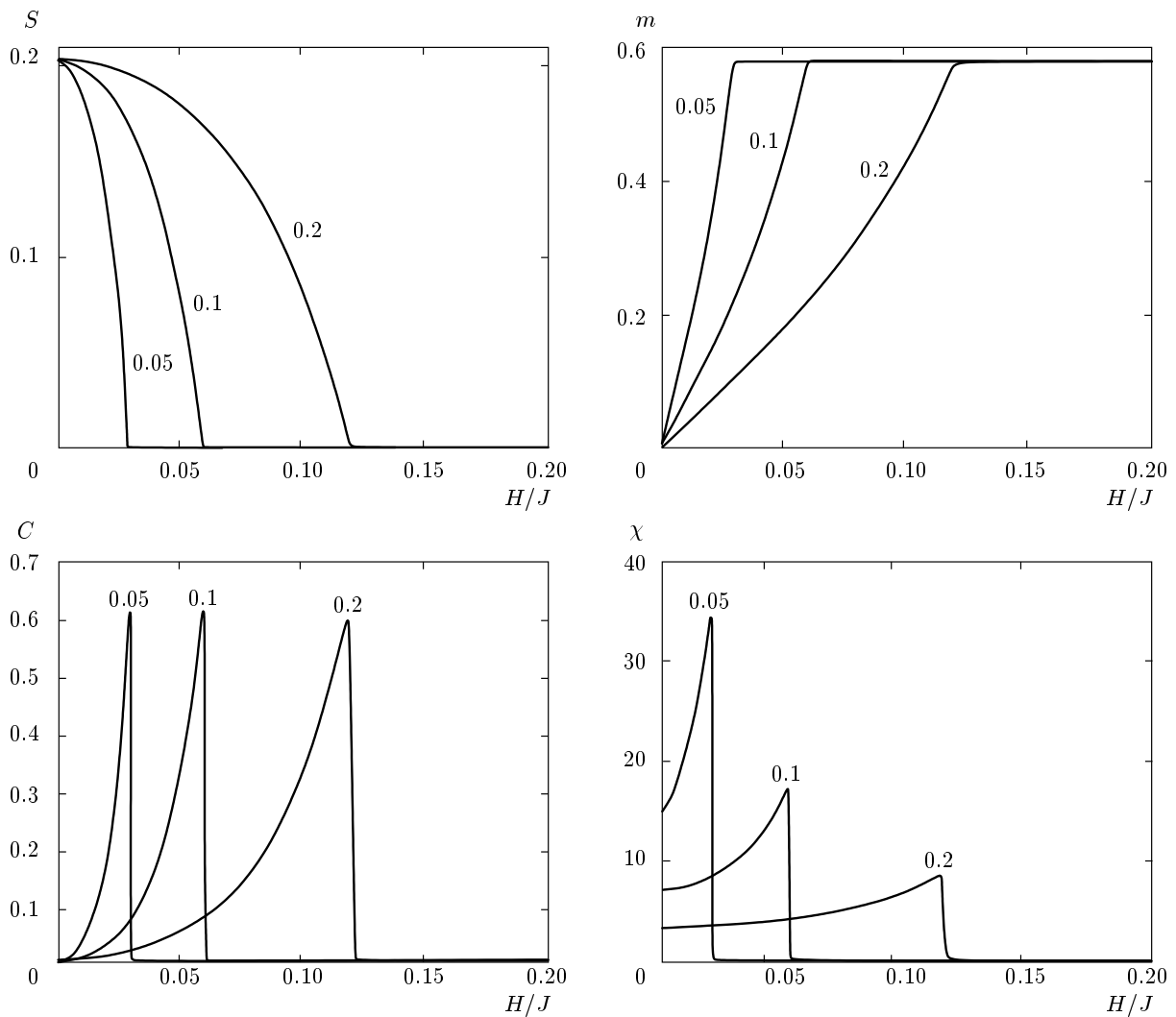


Fig. 10. Field dependences of thermodynamic variables in a [100] field at $T \ll J$. The values of T/J are shown near the curves

At $H = H_c - 0$ ($b = 1/2 + 0$)

$$\chi' = \frac{16}{9}, \quad C = \frac{4}{3} \ln^2 2 \approx 0.64, \quad m = \frac{1}{\sqrt{3}}, \quad S = 0.$$

These expressions agree well with the numerical data for $T \leq 0.2J$ shown in Figs. 9 and 10 and with the results of Monte Carlo simulations [16, 17].

Figure 11 presents the general view of S and C behavior over the H - T plane, and Fig. 12 depicts the location of the specific heat ridges defining the quasi-transitions between paramagnetic, spin ice, and saturated quasi-phases. We note that the dashed line in Fig. 12 does not correspond to a local maximum of C because it vanishes at higher fields; it is only a continuation of the low-field ridge. Therefore, the exact determination of boundaries between “quasi-phases” from

S and C behavior is not always possible. The existing experiments in a [100] field [6, 8, 12] give only scarce evidence in favor of the present results far from the $T = H = 0$ point.

4. SPIN ICE IN THE [011] FIELD

For

$$\mathbf{H} = \frac{H}{\sqrt{2}} (\mathbf{e}_y + \mathbf{e}_z),$$

we have

$$h_0 = -h_1 = \sqrt{\frac{2}{3}} h, \quad h_2 = h_3 = 0, \quad h \equiv \beta H.$$

Therefore, the field in the [011] direction does not act on 2, 3 spins that form the β -chains perpendicular to

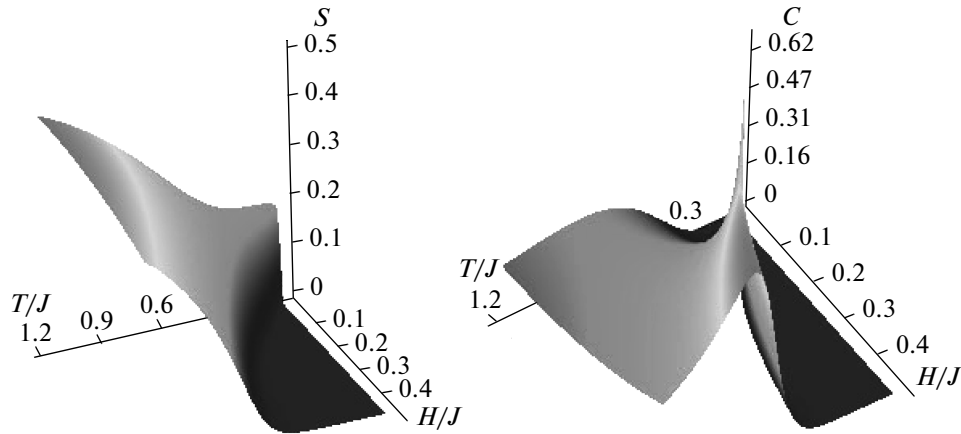


Fig. 11. S and C in a $[100]$ field

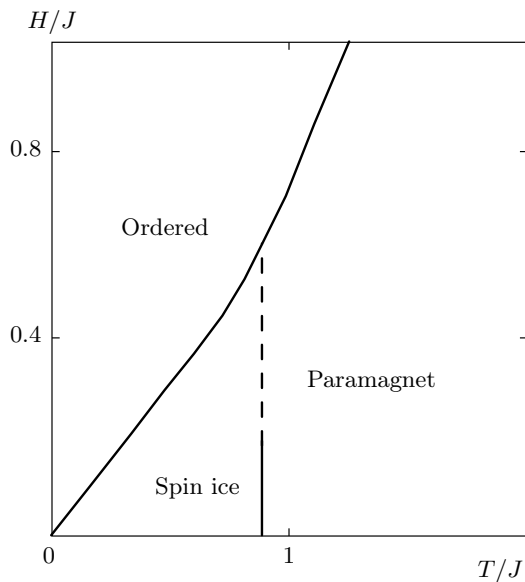


Fig. 12. Pseudo-phases in a $[100]$ field. The dashed line continues the low-field ridge

the field, while 0, 1 spins belong to the α -chains oriented along the field [13]. At $T = 0$, the directions of spins in α -chains are fixed by the field (0 out, 1 in), but the β -chain spins have two possibilities to comply with the spin ice rule and provide the lowest energy: either all 2 spins are fixed at -1 and all 3 spins at $+1$ or vice versa. Hence, for β -chains of a length L , we have $\Gamma = 2^{N/2L}$ ground state configurations. But in spite of the macroscopic degeneracy, the zero-temperature entropy

$$S = \frac{1}{N} \ln \Gamma = \frac{1}{2L} \ln 2$$

tends to zero in the thermodynamic limit. Hence, we here may expect the existence of a crossover between spin ice and “ordered chains” quasi-phases with an increase in the field at low T .

The thermodynamics in such a field is described analytically in a rather simple way. The solution of the equation of state is given by

$$f_0 = -f_1 = x, \quad f_2 = f_3 = 0$$

so

$$\langle \mathbf{m} \rangle = \frac{1}{\sqrt{6}} \operatorname{th} \left(2x - \sqrt{\frac{2}{3}} h \right) \frac{\mathbf{H}}{H},$$

$$Z(x) = 2(1 + e^{-2K}) [\operatorname{ch}(2x) + d(K)],$$

$$d(K) = \frac{1 + 2e^{-2K} + e^{-8K}}{2(1 + e^{-2K})},$$

and the equation of state

$$\operatorname{th} \left(2x - \sqrt{\frac{2}{3}} h \right) [\operatorname{ch}(2x) + d(K)] = \operatorname{sh}(2x)$$

can be easily solved to give

$$m \equiv |\langle \mathbf{m} \rangle| = \frac{1}{\sqrt{6}} \frac{\operatorname{sh} \left(\sqrt{\frac{2}{3}} h \right)}{\sqrt{\operatorname{sh} \left(\sqrt{\frac{2}{3}} h \right)^2 + d^2(K)}}, \quad (41)$$

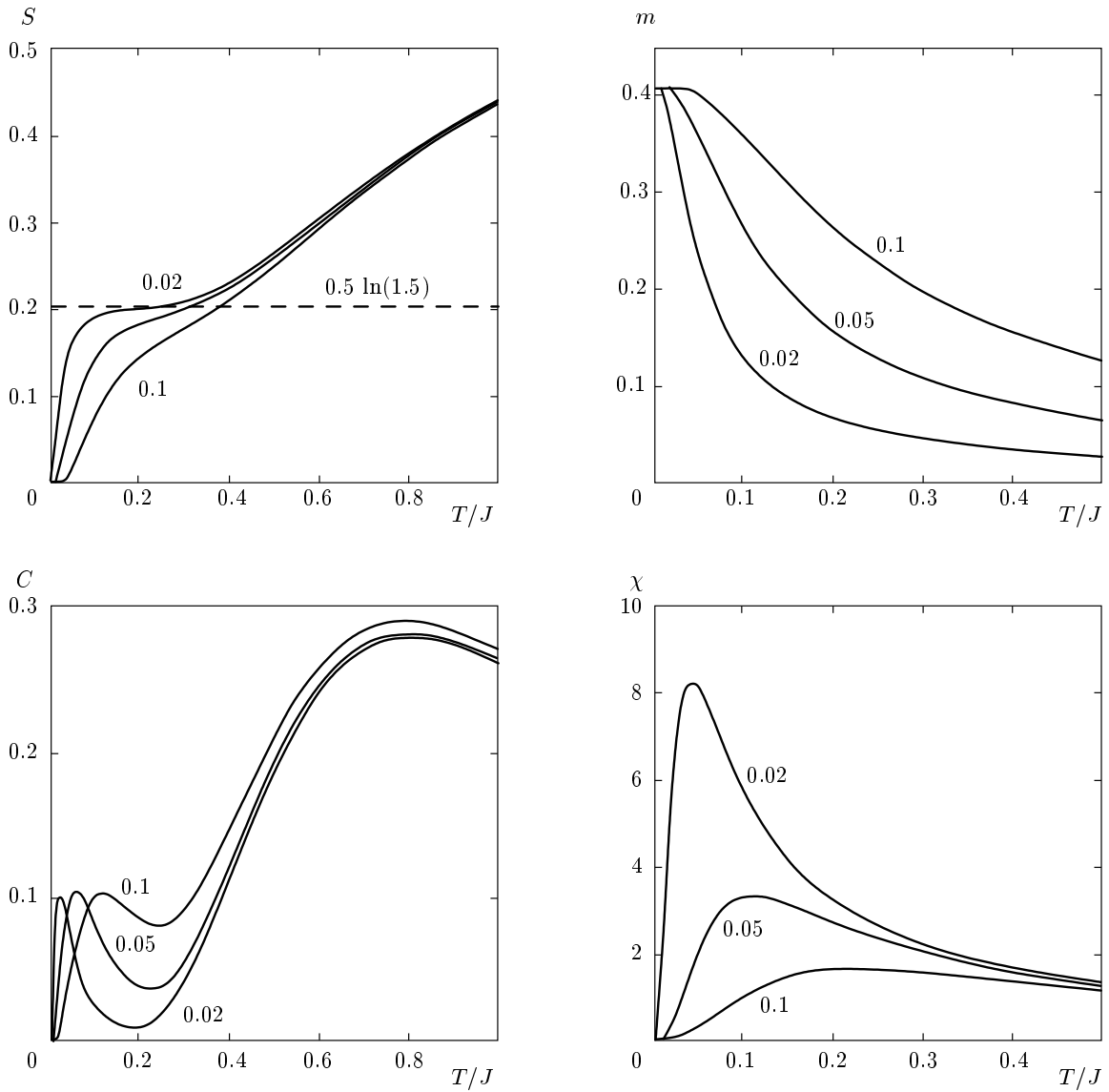


Fig. 13. Temperature dependences of thermodynamic variables in low [011] fields. The values of H/J are shown near the curves. S approaches the Pauling value $S_P = 0.5 \ln(1.5)$ (dashed line) and the low- T peak of C defines the pseudo-transition from spin ice to ordered chains

$$\begin{aligned}
 -2\beta F = & \ln(1 + e^{-2K}) + \\
 & + \ln \left[\operatorname{ch} \left(\sqrt{\frac{2}{3}} h \right) + \sqrt{\operatorname{sh}^2 \left(\sqrt{\frac{2}{3}} h \right) + d^2(K)} \right]. \quad (42)
 \end{aligned}$$

We do not present the general expressions for S , C , and χ here because they are rather cumbersome. But for $T \ll J$, $d(K) \approx 1/2$ and we obtain the following scaling functions of h :

$$m = \sqrt{\frac{2}{3}} \frac{t}{\sqrt{1 + 3t^2}}, \quad t \equiv \operatorname{th} \left(\sqrt{\frac{2}{3}} h \right),$$

$$\begin{aligned}
 -\beta F = & \frac{1}{2} \ln \frac{3}{2} + \frac{1}{2} \ln \frac{\sqrt{1 - t^2}}{2 - \sqrt{1 + 3t^2}}, \quad S = -\beta F - hm, \\
 \chi' \equiv & \frac{\partial m}{\partial h} = \frac{2}{3} \frac{1 - t^2}{(1 + 3t^2)^{3/2}}, \quad C = h^2 \chi'.
 \end{aligned}$$

At $H = 0$, therefore, $S = S_P$, $C = m = 0$, and $\chi' = 2/3$, while at $T = 0$, $S = C = \chi' = 0$ and $m = 1/\sqrt{6} \approx 0.41$. Accordingly, the specific heat $C(T)$ shows a maximum at $T \ll J$ and $H_c \approx 0.86T$, indicating a crossover between spin ice and “ordered chains” quasi-phases in addition to the one at $T \approx 0.8J$ for the paramagnet–spin ice quasi-transition (cf. Fig. 13).

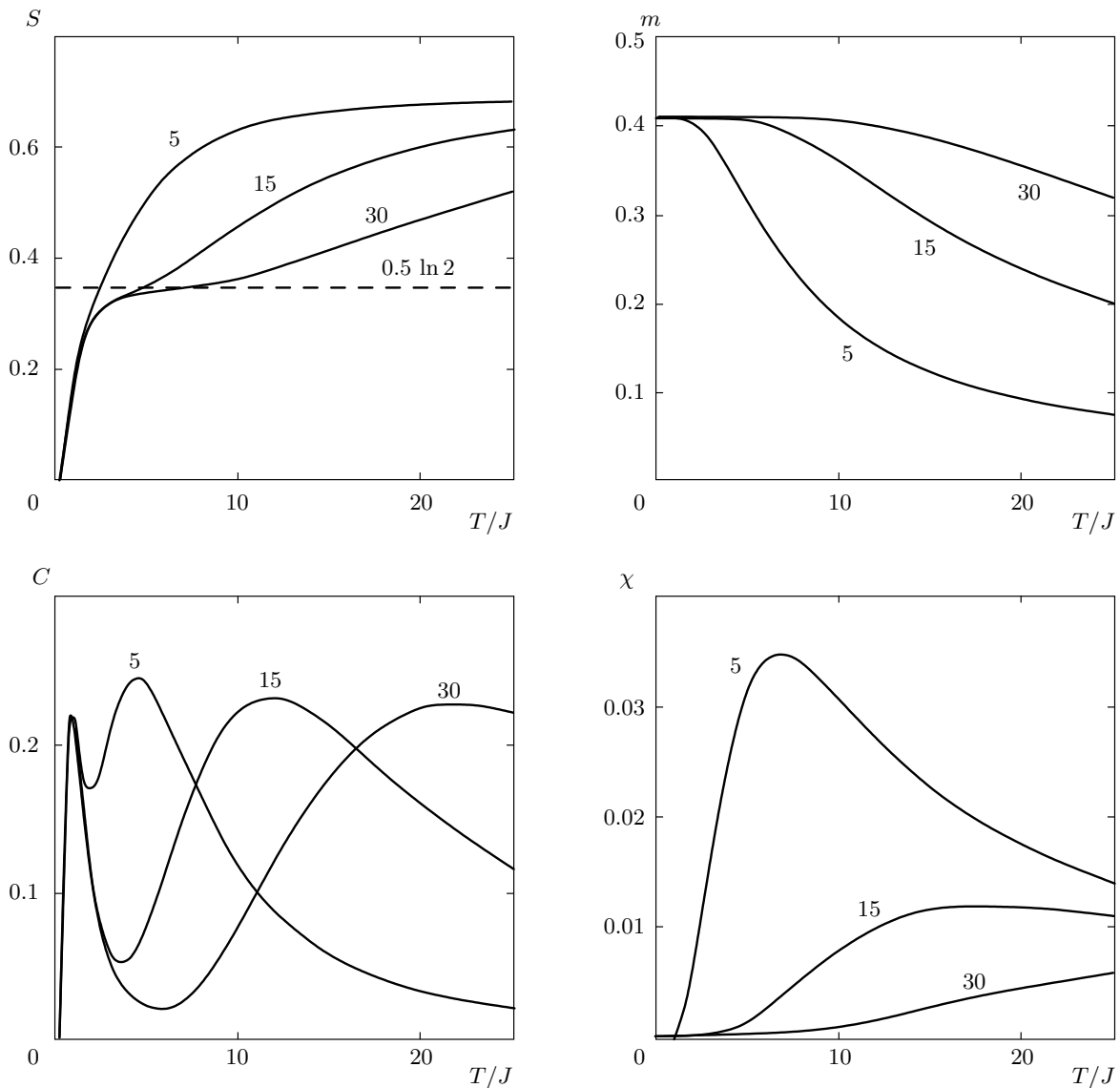


Fig. 14. Temperature dependences of thermodynamic variables in high [011] fields. The values of H/J are shown near the curves. The high-field S approaches the “random β -chain” value $0.5 \ln 2 \approx 0.35$ (dashed line) in the region delimited by C maxima

Another specific quasi-phase exists in a [011] field at $J \ll T \ll H$. Indeed, it follows from (41) and (42) that

$$m = \frac{1}{\sqrt{6}}, \quad -\beta F = \frac{1}{2} \ln 2 + \frac{h}{\sqrt{6}}, \quad S = \frac{1}{2} \ln 2 \approx 0.35.$$

In this region, the strong field fixes the directions of 0, 1 spins, but T is sufficiently high to initiate free flips of spins in β -chains. These flips have no effect on m , which is determined solely by 0, 1 spins, but give rise to half the paramagnetic entropy because half of the spins in a system fluctuate between two states. As a result, we have two maxima of $C(T)$, one at $T \approx 0.8J$ indicating

the crossover between “random β -chains” and “ordered chains” quasi-phases, and the other at $T \approx 0.9H$ corresponding to the “random β -chains”–paramagnet quasi-transition (see Fig. 14).

The overall picture of the $C(T, H)$ relief is shown in Fig. 15. Its ridges are used to define the boundaries between quasi-phases presented in Fig. 16. Again, we have no first-order transitions anticipated on the basis of simulations [12]. The experimental C in a [011] field and the resulting phase diagram [13] agree qualitatively with Figs. 15 and 16 except for the close vicinity of the $H = T = 0$ point.

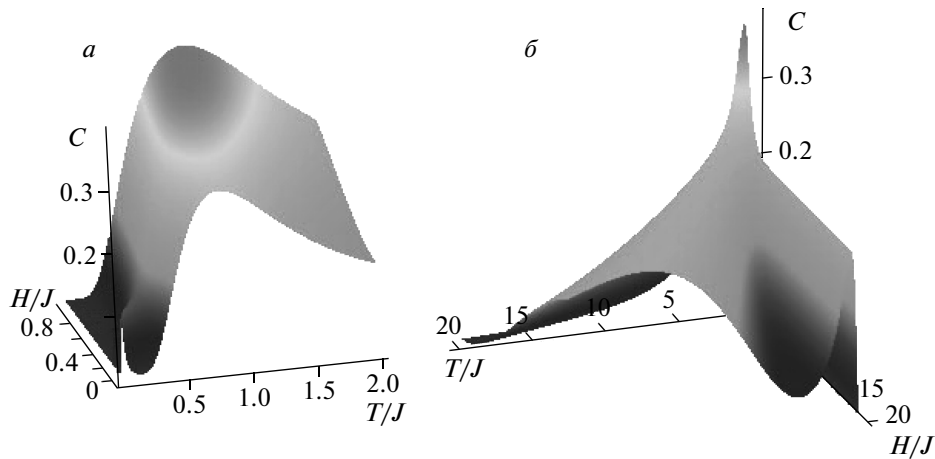


Fig. 15. Specific heat in low (a) and high (b) [011] fields

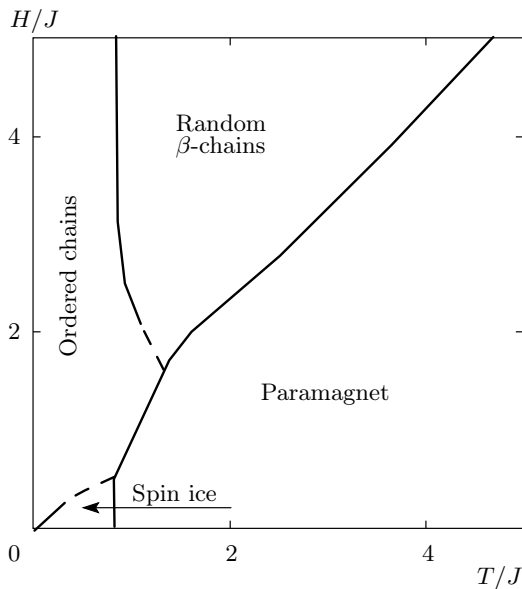


Fig. 16. Pseudo-phases in a [011] field. Dashed lines are the continuation of the vanishing ridges of C

5. CONCLUSIONS

The main conclusion from the present results is that the BP approximation can adequately describe many intricate features of the thermodynamics of a short-range frustrated magnet in a field. In some way, it is superior to the Monte Carlo simulations because it helps discern the true phase transitions and sharp crossovers. In the cases considered in the present model, true first-order transitions occur only at $T = H = 0$ and at $T = 0, H = 6J$ points, while sharp field-induced anomalies result from their proximity. It is quite possi-

ble that this feature is preserved in the rigorous theory of short-range 3D spin ice, because the present results closely resemble the numerically exact Monte Carlo data. More generally, we note that the BP approximation adequately describes the short-range correlations and neglects the long-range ones, and this is sufficient to give a qualitatively correct picture of thermodynamics near first-order transitions where the correlation length stays finite. Evidently, it would be less successful in the vicinity of second-order transitions.

We also note that the BP approximation is a variant of more general cluster variation methods [20, 21], which can give adequate quantitative results for systems with strong short-range competing interactions (in contrast to the simple mean field approximation). In particular, the application of cluster methods to the crystals with tetrahedral units in their structures such as KDP-type ferroelectrics [22] and ordering alloys [21, 23] have also yielded the results that can be compared favorably with those of Monte Carlo simulations. We may therefore suppose that further developing the cluster approximation beyond the BP one along the lines of Refs. [20, 21] could further improve the description of the thermodynamics of spin ice compounds.

Another point demonstrated by the BP results is the usefulness of the notions of “quasi-phases” and “pseudo-transitions”. For example, they relieve us from the necessity to guess what the order parameter for the Kasteleyn transition is or whether it is of the first-order or of the second-order type. They also allow us to discern the definite spin-liquid states even at very high temperatures and fields, which is the case of the “random β -chains” quasi-phase in a [011] field (see Fig. 16).

However, it is not always possible to assign the definite type of spin excitations to a region surrounded by specific heat ridges (cf. Fig. 8), and these ridges may vanish to leave the boundary between quasi-phases indefinite (see Figs. 12 and 16).

The present results also nearly quantitatively reproduce the experimental data for the entropy and magnetization of spin ices in fields. However, experimental results for the specific heat in the vicinity of the mentioned zero-temperature transitions show much less agreement with the theory. The origin of these discrepancies still has to be found in future studies.

Author gratefully acknowledges the useful discussions of this work with S. N. Korshunov.

REFERENCES

1. M. J. Harris, S. T. Bramwell, D. F. McMorrow, T. Zeiske, and K. W. Godfrey, *Phys. Rev. Lett.* **79**, 2554 (1997).
2. A. P. Ramirez, A. Hayashi, R. J. Cava, and R. Sridharthan, *Nature* **399**, 333 (1999).
3. S. V. Isakov, R. Moessner, and S. L. Sondhi, *Phys. Rev. Lett.* **95**, 217201 (2005).
4. M. J. P. Gingras, Spin Ice, arXiv:cond-mat/0903.2772, Lecture Notes for Trieste Summer School, August (2007).
5. O. A. Petrenko, M. R. Lees and G. Balakrishnan, *Phys. Rev. B* **68**, 012406 (2003).
6. H. Fukazawa, R. G. Melko, R. Higashinaka, Y. Maeno, and M. J. P. Gingras, *Phys. Rev. B* **65**, 054410 (2002).
7. T. Fennell, O. A. Petrenko, B. Fak, J. S. Gardner, S. T. Bramwell, and B. Ouladdiaf, *Phys. Rev. B* **72**, 224411 (2005).
8. R. Higashinaka, H. Fukazawa, and Y. Maeno, *Phys. Rev. B* **68**, 014415 (2003).
9. Z. Hiroi, K. Matsuhira, S. Takagi, T. Tayama, and T. Sakakibara, *J. Phys. Soc. Jpn.* **72**, 411 (2003); arXiv:cond-mat/0211326.
10. R. Higashinaka, H. Fukazawa, K. Deguchi, and Y. Maeno, *J. Phys. Soc. Jpn.* **73**, 2845 (2004); arXiv:cond-mat/0406307.
11. T. Sakakibara, T. Tayama, Z. Hiroi, K. Matsuhira, and S. Takagi, *Phys. Rev. Lett.* **90**, 207205 (2003).
12. Shun-ichi Yoshida, Koji Nemoto, and Koh Wada, *J. Phys. Soc. Jpn.* **73**, 1619 (2004); arXiv:cond-mat/0403762.
13. Z. Hiroi, K. Matsuhira, and M. Ogata, *J. Phys. Soc. Jpn.* **72**, 3045 (2003); arXiv:cond-mat/0306240.
14. J. S. Gardner, M. J. P. Gingras, and J. E. Greedan, *Rev. Mod. Phys.* **82**, 53 (2010).
15. J. Villain, *Z. Phys. B* **33**, 31 (1979).
16. M. J. Harris, S. T. Bramwell, P. C. W. Holdsworth, and J. D. M. Champion, *Phys. Rev. Lett.* **81**, 4496 (1998).
17. L. Jaubert, J. T. Chalker, P. C. W. Holdsworth, and R. Moessner, *Phys. Rev. Lett.* **100**, 067207 (2008); arXiv:cond-mat/0710.0976; *J. Phys.: Conf. Series* **145**, 012024 (2009); arXiv:cond-mat/0903.1155.
18. S. V. Isakov, K. S. Raman, R. Moessner, and S. L. Sondhi, *Phys. Rev. B* **70**, 104418 (2004).
19. L. Pauling, *J. Amer. Chem. Soc.* **57**, 2680 (1935); P. W. Anderson, *Phys. Rev.* **102**, 1008 (1956).
20. A. Pelizzola, *J. Phys. A* **38**, R309 (2005).
21. V. G. Vaks and G. D. Samolyuk, *JETP* **115**, 158 (1999).
22. V. G. Vaks, V. I. Zinenko, and V. E. Shneider, *Usp. Fiz. Nauk* **141**, 629 (1983).
23. V. G. Vaks and I. R. Pankratov, *JETP* **124**, 114 (2003).